10-23-2023

The High Pressure Dependence of X-Ray Induced Decomposition of Cadmium Oxalate

Adrian F. Lua Sanchez
University of Nevada, Las Vegas

Petrika Cifligu
University of Nevada, Las Vegas

Marc Graff
University of Nevada, Las Vegas

Michael Pravica
University of Nevada, Las Vegas

Pradip K. Bhowmik
University of Nevada, Las Vegas

RESEARCH ARTICLE | OCTOBER 23 2023

The high pressure dependence of x-ray induced decomposition of cadmium oxalate

Adrian F. Lua Sanchez ; Petrika Cifligu ; Marc Graff; Michael Pravica ; Pradip K. Bhowmik ; Changyong Park ; Egor Evlyukhin

AIP Advances 13, 105031 (2023)
https://doi.org/10.1063/5.0168449

The high pressure dependence of x-ray induced decomposition of cadmium oxalate

Cite as: AIP Advances 13, 105031 (2023); doi: 10.1063/5.0168449
Submitted: 18 July 2023 • Accepted: 3 October 2023 •
Published Online: 23 October 2023

Adrian F. Lua Sanchez,[1] Petrika Cifligu,[1] Marc Graff,[1] Michael Pravica,[1] Pradip K. Bhowmik,[2] Changyong Park,[3] and Egor Evlyukhin[1,a)]

AFFILIATIONS

[1] Department of Physics and Astronomy, University of Nevada Las Vegas, Las Vegas, Nevada 89154, USA
[2] Department of Chemistry and Biochemistry, University of Nevada Las Vegas, Las Vegas, Nevada 89154, USA
[3] High Pressure Collaborative Access Team (HPCAT), X-Ray Science Division, Argonne National Laboratory, Lemont, Illinois 60439, USA

[a)] **Author to whom correspondence should be addressed:** egor.evlyukhin@unlv.edu

ABSTRACT

The high proclivity of x rays to destabilize and distort molecular structures has been previously utilized in the synthesis of novel compounds. Here, we show that x-ray induced decomposition of cadmium oxalate induces chemical and structural transformations only at 0.5 and 1 GPa. Using x-ray diffraction and Raman spectroscopy, the synthesized product is identified as cadmium carbonate with cadmium oxalate remnants, which is stable under ambient conditions. At ambient and >1 GPa pressures, only degradation of the electronic density distribution is observed. The transformation kinetics are examined in terms of Avrami's model, which demonstrates that despite the necessity of high pressure for efficient x-ray induced synthesis of cadmium carbonate, the rate and geometry of structural synthesis in the 0.5–1 GPa pressure range do not depend on the applied pressure. In addition, the possible role of intermolecular distance and molecular mobility in transformation yield is also discussed. Our experimental results indicate that x-ray induced photochemical synthetic pathways can be modulated and optimized by specific parameter selection such as high pressure.

INTRODUCTION

Various interdisciplinary fields of science rely on comprehending the chemical and structural effects caused by x-ray induced stimuli. For example, x rays have been shown to impair the function of vital biological molecules, prominently affecting those with metal centers.[1] Furthermore, x-ray irradiation has been employed to target cancerous cells as a means of radiotherapy.[2,3] In the past several decades, it has been established that the main factors responsible for x-ray induced damage of matter are electronic relaxation processes induced by x-ray photoabsorption. These relaxation cascades exhibit a strong dependence on the chemical environment, initial charge states of atomic entities, atomic/molecular spatial separation, and x-ray energy. Recent studies have shown that the highly ionizing properties of x rays can be utilized to damage simple molecular compounds, resulting in their oxidation state distortion and subsequent disassociation.[4] For instance, these radiation effects have been demonstrated in weakly bound matter (hydrogen or Van der Waals bonding) such as liquids, clusters, and simple molecular gases.[4–6] However, the competitive nature of electronic relaxation cascades, which is based on their probabilistic and ultrafast character, makes the control of their pathways complicated.

It should be noted that x-ray induced distortion and disassociation of molecular structures significantly complicate x-ray crystallographic analysis, especially pertaining to the study of solid-state material structures and properties at high pressure (HP). Indeed, the decomposition of cesium oxalate monohydrate at HP leading to the synthesis of the novel structural form of cesium superoxide via monochromatic x rays has been recently demonstrated.[7,8] Moreover, Goldberger *et al.*[9] showed that gaseous NO_2 and O_2 are produced via x-ray induced damage of barium and strontium nitrate only at ~0.5 GPa. In these studies, it has been proposed that the reduced spatial separation between atomic entities, induced by HP, increases the rate of electronic decay processes, thereby triggering dissociation of initial compounds.

To further investigate the critical role of HP in x-ray induced transformations of powdered solid-state compounds, in this work, we examine the chemical and structural evolution of cadmium oxalate (CdC_2O_4) subjected to monochromatic x rays under ambient and HP conditions. We show the distinct formation of cadmium carbonate ($CdCO_3$) from CdC_2O_4 only at 0.5 and 1 GPa pressure points, which is verified by angular-dispersive x-ray diffraction (XRD) and Raman spectroscopy. Furthermore, the kinetics of transformation in the frame of Avrami's model are investigated to acquire deeper insight into the underlying mechanism of x-ray induced synthesis of $CdCO_3$.

EXPERIMENTAL METHODS

All experiments were performed at the 16 BM-D beamline of the High Pressure Collaborative Access Team (HP-CAT) facilities at the Advanced Photon Source.[10] A tunable Si (111) double crystal in the pseudo-channel-cut mode was used as a monochromator to filter what is labeled as "white" x-ray radiation and deliver x rays of fixed but tunable energies. Symmetric-style diamond anvil cells (DACs) with 250 μm thick stainless-steel gaskets were used to confine and pressurize the samples. All samples were loaded into 120–150 μm diameter holes that were drilled in the gasket center (which were first indented to ~50 μm thickness) using a laser micromachining system located at the HPCAT.[11] Powdered cadmium oxalate (CdC_2O_4) samples (City Chemical LLC, purity >99.9%) were loaded into the DACs under ambient conditions. An ~10 μm diameter ruby sphere was loaded with each sample for pressure measurement purposes, and no pressure transmitting medium was used in any experiments. All samples were irradiated for 1 h with monochromatic x rays at 27 keV energy (λ = 0.4592 Å). The horizontal and vertical full width at half-maximum (FWHM) of the x-ray beam was 4×4.7 μm^2. The corresponding photon flux density was 1.09×10^7 photons/(s μm^2). Angle-dispersive x-ray diffraction patterns were collected every minute during x-ray irradiation using a Pilatus® 1M detector. Afterward, all diffraction patterns were integrated in 2-theta using the Dioptas® program[12] to produce intensity vs 2-theta plots. We note that all measurements were performed at room temperature. In addition, the Raman spectra of the samples loaded in the DACs at RT were measured with an Ar-ion multiline laser (532 nm) in the backscattering configuration using an ISA HR460 spectrometer equipped with a Peltier-cooled Andor® 1024 × 128 pixel^2 CCD detector.

RESULTS AND DISCUSSION

Powdered CdC_2O_4 was loaded into DACs and irradiated with monochromatic x rays. Previously, we have demonstrated that, in the case of cesium oxalate monohydrate ($Cs_2C_2H_2O_5$), the maximum decomposition/transformation yield is achieved when crystalline samples are irradiated with x-ray energy slightly above its cation's K-edge.[8] Thus, the selected 27 keV energy, which is just above the K-edge of cadmium, 26.714 keV,[13] was used to irradiate CdC_2O_4 at ambient and selected HPs (0.5, 1, and 2 GPa). Figure 1 shows the *in situ* XRD patterns of CdC_2O_4 at the studied pressure points after varied x-ray irradiation times. The initial XRD pattern, obtained after one minute of irradiation, for ambient pressure corresponds to the previously reported monoclinic crystal structure of cadmium oxalate with the $P2_1/n$ space group[14] [see vertical bars in Fig. 1(a)]. The other initial XRD patterns recorded at HPs indicate that pressure by itself does not induce formation of a new crystal structure in the 0–2 GPa pressure range (see Fig. S1); however, an observed gradual shift of all XRD peaks toward a higher 2θ implies a reduction in the unit cell volume with applied HP. Every initial XRD pattern was refined to determine the corresponding lattice parameters at ambient and HP, as presented in Table S1 (see the supplementary material). We note that the HP behavior of CdC_2O_4 is consistent with previous studies of oxalate salts at applied HP.[7,8,15] Figures 1(a) and 1(d) show the *in situ* XRD patterns of CdC_2O_4 at ambient and 2 GPa pressure after different x-ray irradiation times, respectively. It is evident that after a full hour of irradiation, only a decrease in peak intensities is observed, the overall XRD peak

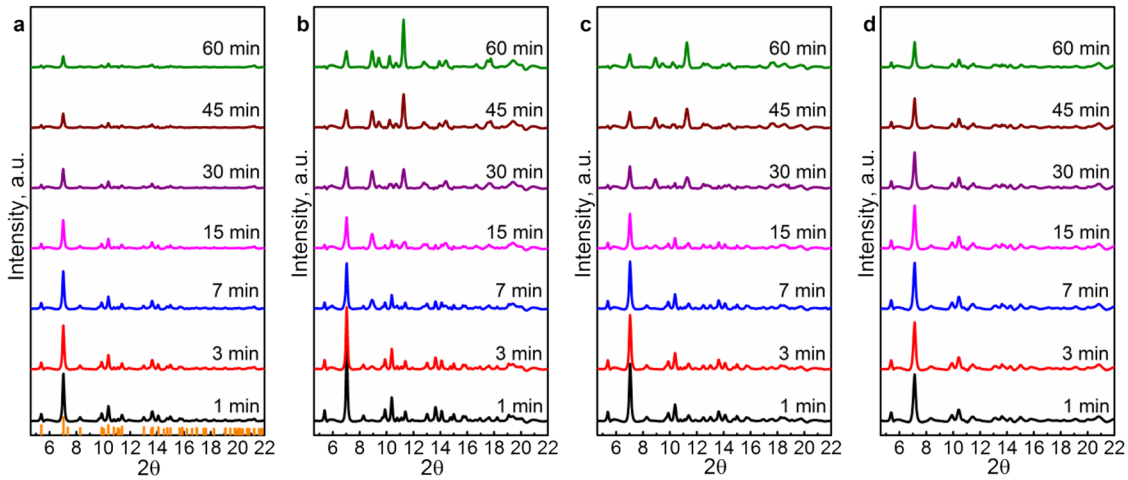

FIG. 1. XRD patterns of cadmium oxalate, irradiated with 27 keV x rays, at different elapsed times. (a) CdC_2O_4 at ambient pressure; vertical bars indicate the peak positions of the previously reported monoclinic crystal structure of cadmium oxalate. (b) CdC_2O_4 at 0.5 GPa. (c) CdC_2O_4 at 1 GPa. (d) CdC_2O_4 at 2 GPa.

positions do not change, and no new peaks are detected. This indicates that monochromatic x rays at ambient pressure and 2 GPa do not induce synthesis of novel crystalline compounds and only result in a distortion of the electron density distribution, as visualized by the 3–60 min patterns in Figs. 1(a) and 1(d). Similar x-ray induced behavior was previously reported for strontium and cesium oxalates as well as for barium and strontium nitrates.[7,9,15] In contrast, when 0.5 or 1 GPa pressures are applied, the response of CdC_2O_4 samples to x rays dramatically changes. As depicted in Fig. 1(b), in 3–7 min at 0.5 GPa, a decrease in the overall peak intensities as well as the appearance of a new peak situated around 8.9° is detected. At 15 min, significant changes in the XRD pattern are observed: two peaks located at 11.1° and 11.39° merge into one at 11.25°, and four new peaks appear around 10.69°, 12.76°, 14.38°, and 16.66°. Continued irradiation for 30 min induces the formation of two new peaks at 10.21° and 13.91°. Eventually, after one hour of irradiation, an additional new peak appears at 9.41°. It is worth mentioning that all new peaks grow in intensity after their initial appearance. Under 1 GPa pressure [as shown in Fig. 1(c)], similar spectroscopic behavior of CdC_2O_4 is observed, albeit, at later irradiation times than 0.5 GPa. Following one hour of irradiation, the final XRD patterns obtained at 0.5 and 1 GPa are completely different from the initial diffraction patterns, implying significant structural changes in CdC_2O_4.

To characterize the chemical composition of the synthesized products, Raman spectroscopic analysis was performed. Figure 2(a) displays a picture of the recovered sample after an hour of irradiation at 0.5 GPa; the black dot corresponds to the damaged area exposed to monochromatic x rays, and the remaining unaffected portion of the sample is the non-irradiated area. In Fig. 2(b), the Raman spectra of both areas are displayed. Six distinct peaks located at 520, 555, 600, 611, 843, and 918 cm^{-1} are found in the Raman spectra of the undamaged region. These spectral features were compared to those identified in natural oxalates.[16] The peaks in the 500–650 cm^{-1} range are attributed to symmetric OCO bending, while the peaks in the 800–1100 cm^{-1} range correspond to the υ (C–C) stretching mode.[16] In comparison, the irradiated (damaged) area has a completely new peak at 1093 cm^{-1} and several significantly reduced peaks from the original sample. Previous studies regarding Raman spectroscopy of various carbonates demonstrated that high intensity peaks in the 1050–1100 cm^{-1} region correspond to a symmetric stretching of a CO_3 group.[17] Therefore, it can be suggested that the synthesized product is $CdCO_3$ with remnants of undecomposed CdC_2O_4.

To verify the x-ray induced chemical reaction pathway, as well as to identify the crystal structure of the obtained compound, an additional assignment of the final XRD pattern obtained at 0.5 GPa with a reported crystal structure of $CdCO_3$[18] was conducted (see Fig. 3). As previously mentioned, the most intense peaks in the final XRD pattern are located at 8.9°, 9.41°, 10.21°, 11.25°, 13.9°, and 14.38°. The positions of these peaks align well with those of the monoclinic structure of $CdCO_3$ with the $R\bar{3}c$ space group[18] (blue vertical bars in Fig. 3). In addition, the final pattern also contains several peaks from the initial XRD pattern positioned at 5.38°, 7°,

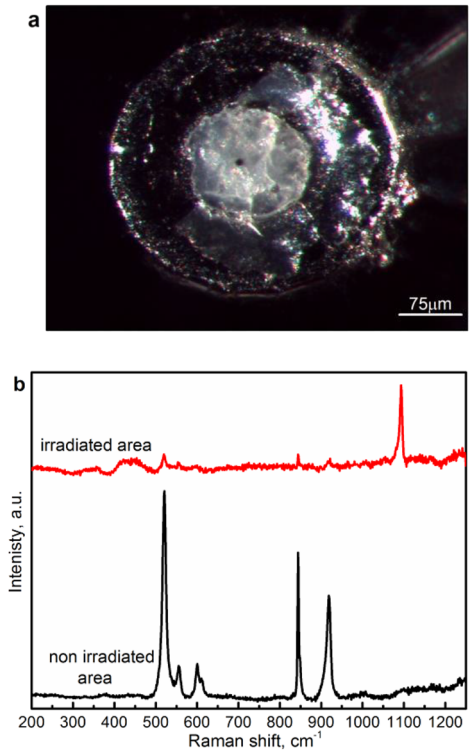

FIG. 2. (a) Picture of the recovered product after being irradiated for 1h. The black dot is the damaged area. (b) Raman spectra of the cadmium oxalate sample pictured in both the damaged area and the surrounding undamaged area.

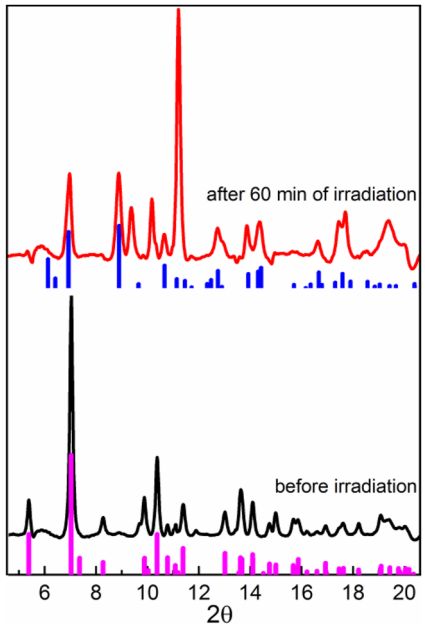

FIG. 3. XRD pattern of cadmium oxalate, CdC_2O_4, at 0.5 GPa before and after irradiation. Purple vertical bars correspond to the previously reported monoclinic crystal structure of CdC_2O_4;[14] blue vertical bars depict the monoclinic crystal structure of cadmium carbonate, $CdCO_3$, reported in Ref. 18.

and 9.8° with significantly reduced intensities. However, all original peaks in the 16°–20° range completely disappear after one hour of x-ray irradiation. These observations together with our Raman spectroscopic analysis confirm that the final product is indeed a mixture of CdC_2O_4 and $CdCO_3$. We note that an extended irradiation time (>1 h) would potentially lead to a complete conversion of CdC_2O_4 into $CdCO_3$, as it was previously reported for cesium oxalate monohydrate.[7,8]

To measure the x-ray induced structural transformation as a function of HP, and to garner more insights into the mechanism of $CdCO_3$ synthesis, we analyzed the CdC_2O_4 transformation yield (TY) at 0.5 and 1 GPa as a function of irradiation time,

$$TY = \frac{Area_t}{Area_0}, \quad (1)$$

where $Area_t$ and $Area_0$ are the integrated areas of the XRD patterns obtained after various irradiation times and after the initial first min of irradiation, respectively. The TYs of CdC_2O_4 at 0.5 and 1 GPa as functions of irradiation time are shown in Fig. 4(a). After 17 min, the TY of CdC_2O_4 undergoes a decrease to 0.685 at a pressure of 0.5 GPa. At 1 GPa, the TY decreases to around 0.646 following 21 min of irradiation. However, after these initial declines, the TY displays an upward trend at both pressures. After a full hour of x-ray irradiation, the TY at 0.5 GPa is ~0.938, whereas at 1 GPa, its value is ~0.763. The observed structural and chemical transformations can be described by the primary mechanism of x-ray-induced damage, which stems from the electronic relaxation processes triggered by x-ray photoabsorption.[5,6,19–22] Essentially, when atoms of a molecular system absorb sufficiently energetic x-ray photons, their core–shell electrons are excited to a bound state or knocked out/ionized to the surrounding environment, and corresponding relaxation cascades are initiated.[19,20,23] The origination and evolution of these relaxation processes are contingent on the chemical composition and interatomic/intermolecular distances.[24–27] As a result, the x-ray irradiated system becomes distorted and destabilized in terms of the oxidation states, and depending on the external conditions (i.e., temperature, pressure, etc.), it undergoes structural and chemical transformations.[7,9,15] It should be emphasized that electronic relaxation processes occur within the femtosecond timescale, and their probabilistic behaviors are highly dependent on the number of absorbed x-ray photons.[23,28] Consequently, the lengthy timescale (minutes to hours) required for the comprehensive transformation of CdC_2O_4 induced by x-ray irradiation at HP can be attributed to the limited number of x-ray photons available in our experimental setup (1.09×10^7 photons/s μm^2). The obtained difference in the final TY values (after 1 h of irradiation) and the overall x-ray induced structural/chemical dynamics of CdC_2O_4 at HPs suggest a critical role of HP in the synthesis of $CdCO_3$.

To determine the effect of HP on the transformation rate (TR) of x-ray induced $CdCO_3$ synthesis, the Avrami model was applied for two regions: (i) the distinct decrease in TY and (ii) subsequent TY growth. In the first region (up to 17 min of irradiation at 0.5 GPa and 21 min at 1 GPa), initial XRD peak intensities attributed to CdC_2O_4 significantly decrease, and a few small peaks of $CdCO_3$ appear [see Figs. 1(b) and 1(c)]. Therefore, the observed TY reduction, seen in Fig. 4(a), can be associated with a decrease in electron density distribution, suggesting that in this region, the decomposition of the initial compound is the most dominant process. In the subsequent x-ray irradiation time (second region), the considerable growth of new XRD peaks indicates that the chemical and structural transformation of CdC_2O_4 into $CdCO_3$ is the prevailing mechanism. The

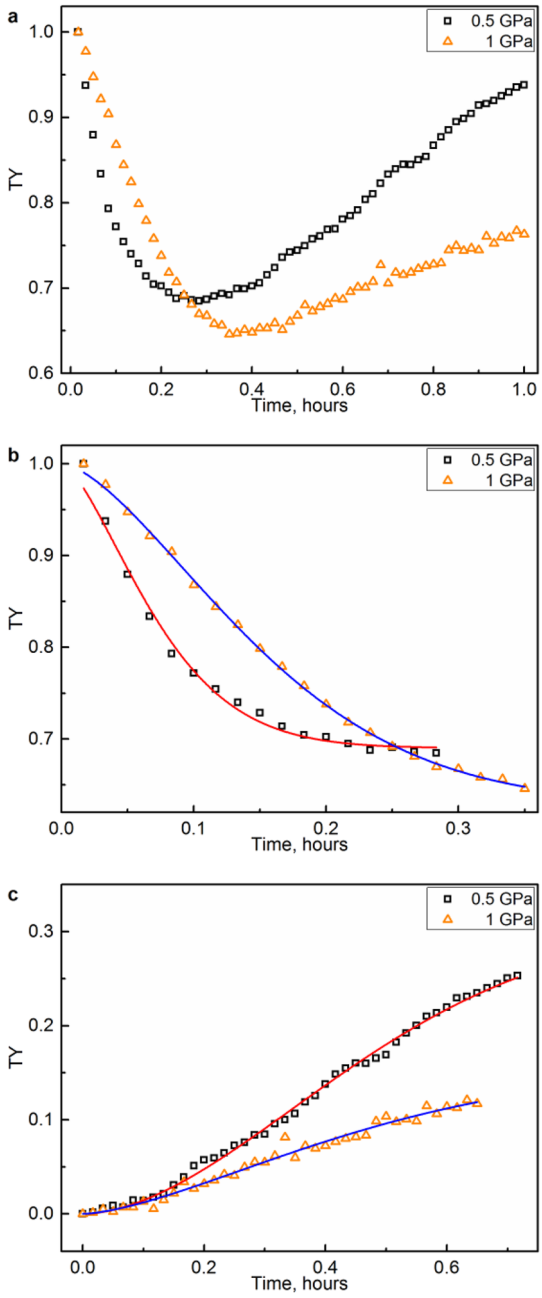

FIG. 4. (a) Transformation yield (TY) of CdC_2O_4 at 0.5 and 1 GPa as a function of x-ray irradiation time. (b) The TY curves in the first region fitted utilizing the modified Avrami equation, which describes the transformation rate of CdC_2O_4. (c) The TY curves in the second region modified to display the beginning of phase transformation and fitted using the general Avrami equation, which describes the transformation rate of $CdCO_3$.

TY curves in the first region were fitted using the following Avrami equation:

$$TY(t) = 1 - [TY_{\infty}(1 - \exp((-kt)^n)]. \quad (2)$$

For the second region,

$$TY(t) = TY_{\infty}(1 - \exp((-kt)^n) \quad (3)$$

where TY(t) and TY_{∞} represent the TY at a specific time "t" and at the end of the selected region, respectively. The variable "k" denotes the rate constant, "t" is the specified time, and "n" is the Avrami exponent whose value is determined by the geometry of the crystalline structure formation.[29] Originally, the Avrami model was developed as a means of describing a phase transformation in solids at constant temperature and later applied for analysis of polymerization processes.[30–33] The equation initially described in this model had some limitations, particularly in accurately evaluating the rate constant "k."[34] Therefore, it was later expanded by Khanna and Taylor where "k" is considered a function of "n,"[35] enabling a more precise analysis of transformation kinetics. We note that the Avrami model was designed to analyze crystalline growth, which produces an upward sigmoid curve. Thus, to properly fit the TY decays in the first region, the modified Avrami equation as expressed by Eq. (2) was used. Figure 4(b) displays the fits of the TY curves at 0.5 and 1 GPa via the modified Avrami equation; the obtained parameters are presented in Table I.

As is evident, the rate constant at 0.5 GPa is 11.93 h^{-1}, nearly twice that at 1 GPa, and the Avrami exponent for both pressure points are ~1.5, suggesting that the mechanism of decomposition is diffusion-controlled.[36] It should be noted that a higher molecular mobility facilitates diffusion processes.[37] Therefore, the drastic difference in the rate constants at both pressure points can be attributed to the reduction in molecular mobility with increasing pressure.[38–42] The values of TY_{∞} obtained from the fits at 0.5 and 1 GPa demonstrate that a ~30% reduction in initial electron density distribution is required before the x-ray induced structural formation $CdCO_3$ becomes dominant.

The TY curves in the second region were fitted via Eq. (3) (general Avrami equation), and the obtained parameters are listed in Table II.

TABLE I. Modified Avrami equation parameters k, n, and TY_{∞} obtained from the fit of CdC_2O_4 decomposition kinetics at 0.5 and 1 GPa in the first region.

Pressure (GPa)	k (h^{-1})	n	TY_{∞}
0.5	11.93 ± 0.41	1.49 ± 0.1	0.31 ± 0.005
1.0	5.70 ± 0.11	1.56 ± 0.3	0.37 ± 0.005

TABLE II. Avrami equation parameters k, n, and TY_{∞} obtained from the fit of CdC_2O_4 decomposition kinetics at 0.5 and 1 GPa in the second region.

Pressure (GPa)	k (h^{-1})	n	TY_{∞}
0.5	1.54 ± 0.11	1.65 ± 0.05	0.295 ± 0.025
1.0	1.94 ± 0.32	1.54 ± 0.13	0.156 ± 0.022

It should be mentioned that in the Avrami model, the beginning of transformation is considered to occur at t = 0, when the studied molecular system is in its initial structural phase. In our case, we recognize that the structural $CdCO_3$ formation becomes dominant after the initial decline in TY curves observed at both pressure points. Therefore, to properly apply the Avrami model, t = 0 for both curves was selected at their lowest TY values; thus, these TY values, along with the time at which they occurred (0.685 and 17 min for 0.5 GPa; 0.646 and 21 min for 1 GPa), were subtracted [see Fig. 4(c)]. As presented in Table II, the rate constant "k" at 1 GPa is slightly larger than that at 0.5 GPa. Their respective "n" values are similar to and are consistent with the "n" values obtained for the first region, suggesting a diffusion-controlled transformation growth.[36] The only striking difference between the TY evolution at both pressure points is the values of the final TY (after one hour of x-ray irradiation). We note that the rates and efficiency of electronic relaxation processes (which are the main factors of x-ray induced damage) depend on the interatomic/intermolecular distances.[43–45] Particularly, at smaller spatial separations, electron transfer processes dominate over the energy transfer decays.[43,46] Moreover, production of slow electrons accompanies all relaxation processes, and their presence within a chemical environment can further destabilize the molecular system via activation of additional radiative/non-radiative electron capture processes.[47,48] Therefore, it can be suggested that at higher pressures, structural and chemical transformations would be more efficient, which is consistent with the observed XRD pattern evolutions at ambient and higher pressures (see Fig. 1). However, reduced molecular mobility due to increasingly higher pressures may restrict formation of $CdCO_3$ (i.e., the x-ray distorted CdC_2O_4 system is unable to efficiently restructure itself) and explain the difference between TY_{∞} at 1–0.5 GPa as well as the absence of any structural transformations at 2 GPa [Fig. 1(d)].

X-ray-induced stimuli present an intriguing dynamic wherein both constructive and destructive processes appear to compete for prominence. The optimization of x-ray-based photochemical synthetic methods could potentially be beneficial for various applications, such as catalytic technologies,[49] adaptive oxide electronics, and optoelectronics,[50–54] where synthesis of novel compounds as well as the formation of their unique structural forms is required. Therefore, conducting additional studies would provide further insights into the dynamics of electronic relaxation processes triggered by x rays and potentially separate these competing mechanisms, offering a more comprehensive understanding of how to optimize the synthesis of compounds (e.g., $CdCO_3$). A potential technique that may assist with this endeavor utilizes X-ray Free-Electron Laser (XFEL), which uses short (femtosecond), intense x-ray pulses.[55] In addition, cold-target recoil-ion-momentum spectroscopy (COLTRIMS) may be suitable in such experiments to avoid issues with the background of scattered secondary electrons.[56] These techniques have been successfully employed in studying gaseous iodine compounds and water dimers/clusters.[46,57,58] We also note that $CdCO_3$ serves as a critical precursor for cadmium-based semiconductors used in photovoltaic technologies,[59] is integral in the formulation of pigments for paints and plastics, and finds essential application in electroplating processes for protective coating.[60–62] Therefore, a novel means of $CdCO_3$ synthesis, presented in this work, could potentially be beneficial in

industrial and environmental applications,[63] which rely on cadmium utilization.

In this study, we have demonstrated that the decomposition of CdC_2O_4 by x rays leads to chemical and structural changes only at pressures of 0.5 and 1 GPa. The resulting product was identified as $CdCO_3$ with a small presence of undecomposed CdC_2O_4, via XRD and Raman spectroscopic analysis. The synthesized compound is fully recoverable and remains stable under normal conditions. We observed that at ambient pressure and pressures exceeding 1 GPa, only degradation of electronic density distribution occurs. By examining the transformation kinetics according to the Avrami model, we have determined that the rate and the geometry of x-ray-induced synthesis of $CdCO_3$ do not depend on the applied high pressure within the 0.5–1 GPa pressure range; however, the maximum TY value was observed at 0.5 GPa. The potential role of reduced spatial separation between molecular entities as well as its correlation with the efficiency of electronic relaxation processes responsible for the transformation of $CdCO_3$ is studied. In addition, restricted molecular mobility caused by HP is proposed as the main factor contributing to the absence of $CdCO_3$ formation at 2 GPa. Our experimental findings suggest that x-ray–matter interaction can be controlled by selectively adjusting parameters such as high pressure and directed toward the synthesis of novel compounds.

SUPPLEMENTARY MATERIAL

See the supplementary material for (S1) the initial XRD patterns of cadmium oxalate (CdC_2O_4) at various pressure points and (Table S1) their corresponding lattice parameters.

ACKNOWLEDGMENTS

We gratefully acknowledge the support from the U. S. Department of Energy, the Basic Energy Sciences (BES) Program, under Award No. DE-SC0023248. This work was performed at HPCAT (Sector 16), Advanced Photon Source (APS), Argonne National Laboratory. HPCAT operations are supported by DOE-NNSA's Office of Experimental Sciences. The Advanced Photon Source is a U.S. Department of Energy (DOE) Office of Science User Facility operated for the DOE Office of Science by Argonne National Laboratory, under Contract No. DE-AC02-06CH11357. E.E. and P.K.B. sincerely acknowledge the financial support of an industrial sponsored project supported by Kosher, Las Vegas, USA. The publication fees for this article were supported by the UNLV University Libraries Open Article Fund.

AUTHOR DECLARATIONS

Conflict of Interest

The authors have no conflicts to disclose.

Author Contributions

Adrian F. Lua Sanchez: Data Curation (supporting); Formal Analysis (supporting); Investigation (equal); Visualization (equal); Writing – original draft (supporting). **Petrika Cifligu**: Conceptualization (supporting); Investigation (equal). **Marc Graff**: Investigation (equal). **Michael Pravica**: Conceptualization (supporting); Project Administration (equal); Resources (equal); Investigation (equal); Supervision (equal); Writing – review & editing (equal). **Pradip K. Bhowmik**: Conceptualization (supporting); Writing – review & editing (equal). **Changyong Park**: Resources (equal); Investigation (equal); Writing – review & editing (equal). **Egor Evlyukhin**: Conceptualization (lead); Data Curation (lead); Formal Analysis (lead); Project Administration (equal); Investigation (equal); Supervision (equal); Visualization (equal); Writing – original draft (lead).

DATA AVAILABILITY

The data that support the findings of this study are available from the corresponding author upon reasonable request.

REFERENCES

[1] H. H. Jawad and D. E. Watt, "Physical mechanism for inactivation of metalloenzymes by characteristic x-rays," Int. J. Radiat. Biol. Relat. Stud. Phys., Chem. Med. **50**(4), 665–674 (1986).
[2] J. Rousseau, C. Boudou, R. F. Barth, J. Balosso, F. Estève, and H. Elleaume, "Enhanced survival and cure of F98 Glioma–bearing rats following intracerebral delivery of carboplatin in combination with photon irradiation," Clin. Cancer Res. **13**(17), 5195–5201 (2007).
[3] R. F. Martin and L. E. Feinendegen, "The quest to exploit the Auger effect in cancer radiotherapy—A reflective review," Int. J. Radiat. Biol. **92**(11), 617–632 (2016).
[4] V. Averbukh, I. B. Müller, and L. S. Cederbaum, "Mechanism of interatomic coulombic decay in clusters," Phys. Rev. Lett. **93**(26), 263002 (2004).
[5] O. Marsalek, C. G. Elles, P. A. Pieniazek, E. Pluhařová, J. VandeVondele, S. E. Bradforth, and P. Jungwirth, "Chasing charge localization and chemical reactivity following photoionization in liquid water," J. Chem. Phys. **135**(22), 224510 (2011).
[6] A. Hans, V. Stumpf, X. Holzapfel, F. Wiegandt, P. Schmidt, C. Ozga, P. Reiß, L. B. Ltaief, C. Küstner-Wetekam, T. Jahnke, A. Ehresmann, P. V. Demekhin, K. Gokhberg, and A. Knie, "Direct evidence for radiative charge transfer after inner-shell excitation and ionization of large clusters," New J. Phys. **20**(1), 012001 (2018).
[7] E. Evlyukhin, P. Cifligu, M. Pravica, P. K. Bhowmik, E. Kim, D. Popov, and C. Park, "Experimental demonstration of necessary conditions for x-ray induced synthesis of cesium superoxide," Phys. Chem. Chem. Phys. **25**(3), 1799–1807 (2023).
[8] E. Evlyukhin, E. Kim, D. Goldberger, P. Cifligu, S. Schyck, P. F. Weck, and M. Pravica, "High-pressure-assisted x-ray-induced damage as a new route for chemical and structural synthesis," Phys. Chem. Chem. Phys. **20**(28), 18949–18956 (2018).
[9] D. Goldberger, C. Park, E. Evlyukhin, P. Cifligu, and M. Pravica, "Cationic dependence of x-ray induced damage in strontium and barium nitrate," J. Phys. Chem. A **122**(44), 8722–8728 (2018).
[10] A. Bommannavar, P. Chow, R. Ferry, R. Hrubiak, F. Humble, C. Kenney-Benson, M. Lv, Y. Meng, C. Park, D. Popov, E. Rod, M. Somayazulu, G. Shen, D. Smith, J. Smith, Y. Xiao, and N. Velisavljevic, "Overview of HPCAT and capabilities for studying minerals and various other materials at high-pressure conditions," Phys. Chem. Miner. **49**(9), 36 (2022).
[11] R. Hrubiak, S. Sinogeikin, E. Rod, and G. Shen, "The laser micro-machining system for diamond anvil cell experiments and general precision machining applications at the High Pressure Collaborative Access Team," Rev. Sci. Instrum. **86**(7), 072202 (2015).
[12] C. Prescher and V. B. Prakapenka, "DIOPTAS: A program for reduction of two-dimensional x-ray diffraction data and data exploration," High Pressure Res. **35**(3), 223–230 (2015).
[13] G. Genchi, M. S. Sinicropi, G. Lauria, A. Carocci, and A. Catalano, "The effects of cadmium toxicity," Int. J. Environ. Res. Public Health **17**(11), 3782 (2020).
[14] E. Jeanneau, N. Audebrand, and D. Louër, "β-CdC_2O_4," Acta Crystallogr., Sect. C: Cryst. Struct. Commun. **57**(9), 1012–1013 (2001).

[15]E. Evlyukhin, E. Kim, P. Cifligu, D. Goldberger, S. Schyck, B. Harris, S. Torres, G. R. Rossman, and M. Pravica, "Synthesis of a novel strontium-based wide-bandgap semiconductor via x-ray photochemistry under extreme conditions," J. Mater. Chem. C **6**(46), 12473–12478 (2018).
[16]R. L. Frost, "Raman spectroscopy of natural oxalates," Anal. Chim. Acta **517**(1–2), 207–214 (2004).
[17]N. Buzgar and A. Apopei, "The Raman study of certain carbonates," Anal. Ştt. Univ. Al. I. Cuza, Sec. II **55**, 97–112 (2009).
[18]F. A. Bromiley, T. B. Ballaran, F. Langenhorst, and F. Seifert, "Order and miscibility in the otavite–magnesite solid solution," Am. Mineral. **92**(5–6), 829–836 (2007).
[19]K. Gokhberg, P. Kolorenč, A. I. Kuleff, and L. S. Cederbaum, "Site- and energy-selective slow-electron production through intermolecular Coulombic decay," Nature **505**(7485), 661–663 (2014).
[20]F. Trinter, M. S. Schöffler, H.-K. Kim, F. P. Sturm, K. Cole, N. Neumann, A. Vredenborg, J. Williams, I. Bocharova, R. Guillemin, M. Simon, A. Belkacem, A. L. Landers, Th. Weber, H. Schmidt-Böcking, R. Dörner, and T. Jahnke, "Resonant Auger decay driving intermolecular Coulombic decay in molecular dimers," Nature **505**(7485), 664–666 (2014).
[21]J. Zobeley, R. Santra, and L. S. Cederbaum, "Electronic decay in weakly bound heteroclusters: Energy transfer versus electron transfer," J. Chem. Phys. **115**(11), 5076–5088 (2001).
[22]O. Carugo and K. D. Carugo, "When x-rays modify the protein structure: Radiation damage at work," Trends Biochem. Sci. **30**(4), 213–219 (2005).
[23]V. Stumpf, K. Gokhberg, and L. S. Cederbaum, "The role of metal ions in x-ray-induced photochemistry," Nat. Chem. **8**(3), 237–241 (2016).
[24]T. Jahnke, H. Sann, T. Havermeier, K. Kreidi, C. Stuck, M. Meckel, M. Schöffler, N. Neumann, R. Wallauer, S. Voss, A. Czasch, O. Jagutzki, A. Malakzadeh, F. Afaneh, T. Weber, H. Schmidt-Böcking, and R. Dörner, "Ultrafast energy transfer between water molecules," Nat. Phys. **6**(2), 139–142 (2010).
[25]S. Yan, P. P. Zhang, V. Stumpf, K Gokhberg, X. C. Zhang, S. Xu, B. Li, L. L. Shen, X. L. Zhu, W. T. Feng, S. F. Zhang, D. M. Zhao, and X. Ma, "Interatomic relaxation processes induced in neon dimers by electron-impact ionization," Phys. Rev. A **97**(1), 10701 (2018).
[26]P. E. Barran, N. R. Walker, and A. J. Stace, "Competitive charge transfer reactions in small $[Mg(H_2O)N]^{2+}$ clusters," J. Chem. Phys. **112**(14), 6173–6177 (2000).
[27]O. Svoboda, D. Hollas, M. Ončák, and P. Slavíček, "Reaction selectivity in an ionized water dimer: Nonadiabatic ab initio dynamics simulations," Phys. Chem. Chem. Phys. **15**(27), 11531–11542 (2013).
[28]A. I. Kuleff, K. Gokhberg, S. Kopelke, and L. S. Cederbaum, "Ultrafast interatomic electronic decay in multiply excited clusters," Phys. Rev. Lett. **105**(4), 043004 (2010).
[29]P. Zemenová, R. Král, M. Rodová, K. Nitsch, and M. Nikl, "Calculations of Avrami exponent and applicability of Johnson–Mehl–Avrami model on crystallization in $Er:LiY(PO_3)_4$ phosphate glass," J. Therm. Anal. Calorim. **141**(3), 1091–1099 (2020).
[30]J. N. Hay, "Application of the modified avrami equations to polymer crystallisation kinetics," Br. Polym. J. **3**, 74–82 (1971).
[31]E. Evlyukhin, L. Museur, M. Traore, S. M. Nikitin, A. Zerr, and A. Kanaev, "Laser-Assisted high-pressure-induced polymerization of 2-(hydroxyethyl)methacrylate," J. Phys. Chem. B **119**(8), 3577–3582 (2015).
[32]M. Avrami, "Granulation, phase change, and microstructure kinetics of phase change. III," J. Chem. Phys. **9**(2), 177–184 (2004).
[33]M. Avrami, "Kinetics of phase change. II. Transformation-time relations for random distribution of nuclei," J. Chem. Phys. **8**(2), 212–224 (2004).
[34]J. N. Hay and Z. J. Przekop, "On a nonexponential transformation equation for spherulitic crystallization," J. Polym. Sci., Polym. Phys. Ed. **16**(1), 81–89 (1978).
[35]Y. P. Khanna and T. J. Taylor, "Comments and recommendations on the use of the Avrami equation for physico-chemical kinetics," Polym. Eng. Sci. **28**(16), 1042–1045 (1988).
[36]C. G. Baek, M. Kim, O. H. Kwon, H. W. Choi, and Y. S. Yang, "Formation of $Ba_2NaNb_5O_{15}$ crystal and crystallization kinetics in $BaO–Na_2O–Nb_2O_5–SiO_2–B_2O_3$Glass," Cryst. Growth Des. **17**(11), 5684–5690 (2017).
[37]M. Rams-Baron, Z. Wojnarowska, K. Grzybowska, M. Dulski, J. Knapik, K. Jurkiewicz, W. Smolka, W. Sawicki, A. Ratuszna, and M. Paluch, "Toward a better understanding of the physical stability of amorphous anti-inflammatory agents: The roles of molecular mobility and molecular interaction patterns," Mol. Pharm. **12**(10), 3628–3638 (2015).
[38]K. Adrjanowicz, A. Grzybowski, K. Grzybowska, J. Pionteck, and M. Paluch, "Effect of high pressure on crystallization kinetics of van der Waals liquid: An experimental and theoretical study," Cryst. Growth Des. **14**(5), 2097–2104 (2014).
[39]I. Gutzow, B. Durschang, and C. Russel, "Crystallization of glassforming melts under hydrostatic pressure and shear stress: Part I crystallization catalysis under hydrostatic pressure: Possibilities and limitations," J. Mater. Sci. **32**(20), 5389–5403 (1997).
[40]S. Schyck, E. Evlyukhin, E. Kim, and M. Pravica, "High pressure behavior of mercury difluoride (HgF_2)," Chem. Phys. Lett. **724**, 35–41 (2019).
[41]E. Evlyukhin, L. Museur, M. Traore, C. Perruchot, A. Zerr, and A. Kanaev, "A new route for high-purity organic materials: High-pressure-ramp-induced ultrafast polymerization of 2-(hydroxyethyl)methacrylate," Sci. Rep. **5**(1), 18244 (2015).
[42]W. Grochala, R. Hoffmann, J. Feng, and N. W. Ashcroft, "The chemical imagination at work in very tight places," Angew. Chem., Int. Ed. **46**(20), 3620–3642 (2007).
[43]T. Jahnke, A. Czasch, M. Schöffler, S. Schössler, M. Käsz, J. Titze, K. Kreidi, R. E. Grisenti, A. Staudte, O. Jagutzki, L. Ph. H. Schmidt, Th. Weber, H. Schmidt-Böcking, K. Ueda, and R. Dörner, "Experimental separation of virtual photon exchange and electron transfer in interatomic coulombic decay of neon dimers," Phys. Rev. Lett. **99**(15), 153401 (2007).
[44]S. Marburger, O. Kugeler, U. Hergenhahn, and T. Möller, "Experimental evidence for interatomic coulombic decay in Ne clusters," Phys. Rev. Lett. **90**(20), 203401 (2003).
[45]G. Öhrwall, M. Tchaplyguine, M. Lundwall, R. Feifel, H. Bergersen, T. Rander, A. Lindblad, J. Schulz, S. Peredkov, S. Barth, S. Marburger, U. Hergenhahn, S. Svensson, and O. Björneholm, "Femtosecond interatomic coulombic decay in free neon clusters: Large lifetime differences between surface and bulk," Phys. Rev. Lett. **93**(17), 173401 (2004).
[46]R. Santra, J. Zobeley, and L. S. Cederbaum, "Electronic decay of valence holes in clusters and condensed matter," Phys. Rev. B **64**(24), 245104 (2001).
[47]K. Gokhberg and L. S. Cederbaum, "Environment assisted electron capture," J. Phys.: Conf. Ser. **388**(6), 062031 (2012).
[48]C. Müller, A. B. Voitkiv, J. R. C. López-Urrutia, and Z. Harman, "Strongly enhanced recombination via two-center electronic correlations," Phys. Rev. Lett. **104**(23), 233202 (2010).
[49]J. C. Védrine, "Importance, features and uses of metal oxide catalysts in heterogeneous catalysis," Chin. J. Catal. **40**(11), 1627–1636 (2019).
[50]G. J. Páez Fajardo, S. A. Howard, E. Evlyukhin, M. J. Wahila, W. R. Mondal, M. Zuba, J. E. Boschker, H. Paik, D. G. Schlom, J. T. Sadowski, S. A. Tenney, B. Reinhart, W.-C. Lee, and L. F. J. Piper, "Structural phase transitions of NbO_2: Bulk versus surface," Chem. Mater. **33**(4), 1416–1425 (2021).
[51]J. L. Andrews, D. A. Santos, M. Meyyappan, R. S. Williams, and S. Banerjee, "Building brain-inspired logic circuits from dynamically switchable transition-metal oxides," Trends Chem. **1**(8), 711–726 (2019).
[52]S. A. Howard, E. Evlyukhin, G. Páez Fajardo, H. Paik, D. G. Schlom, and L. F. J. Piper, "Digital tuning of the transition temperature of epitaxial VO_2 thin films on MgF_2 substrates by strain engineering," Adv. Mater. Interfaces **8**(9), 2001790 (2021).
[53]X. Yu, T. J. Marks, and A. Facchetti, "Metal oxides for optoelectronic applications," Nat. Mater. **15**(4), 383–396 (2016).
[54]W. R. Mondal, E. Evlyukhin, S. A. Howard, G. J. Paez, H. Paik, D. G. Schlom, L. F. J. Piper, and W.-C. Lee, "Role of V–V dimers on structural, electronic, magnetic, and vibrational properties of VO_2 by first-principles simulations and Raman spectroscopic analysis," Phys. Rev. B **103**(21), 214107 (2021).
[55]U. Bergmann, J. Kern, R. W. Schoenlein, P. Wernet, V. K. Yachandra, and J. Yano, "Using x-ray free-electron lasers for spectroscopy of molecular catalysts and metalloenzymes," Nat. Rev. Phys. **3**(4), 264–282 (2021).
[56]R. Dörner, V. Mergel, L. Spielberger, O. Jagutzki, M. Unverzagt, W. Schmitt, J. Ullrich, R. Moshammer, H. Khemliche, M. Prior, R. E. Olson, L. Zhaoyuan,

W. Wu, C. L. Cocke, and H. Schmidt-Böcking, "Cold target recoil ion momentum spectroscopy," AIP Conf. Proc. **360**(1), 495–504 (1996).
[57]M. Mucke, M. Braune, S. Barth, M. Förstel, T. Lischke, V. Ulrich, T. Arion, U. Becker, A. Bradshaw, and U. Hergenhahn, "A hitherto unrecognized source of low-energy electrons in water," Nat. Phys. **6**(2), 143–146 (2010).
[58]R. Boll, J. M. Schäfer, B. Richard, K. Fehre, G. Kastirke, Z. Jurek, M. S. Schöffler, M. M. Abdullah, N. Anders, T. M. Baumann, S. Eckart, B. Erk, A. De Fanis, R. Dörner, S. Grundmann, P. Grychtol, A. Hartung, M. Hofmann, M. Ilchen, L. Inhester, C. Janke, R. Jin, M. Kircher, K. Kubicek, M. Kunitski, X. Li, T. Mazza, S. Meister, N. Melzer, J. Montano, V. Music, G. Nalin, Y. Ovcharenko, C. Passow, A. Pier, N. Rennhack, J. Rist, D. E. Rivas, D. Rolles, I. Schlichting, L. Ph.H. Schmidt, P. Schmidt, J. Siebert, N. Strenger, D. Trabert, F. Trinter, I. Vela-Perez, R. Wagner, P. Walter, M. Weller, P. Ziolkowski, S.-K. Son, A. Rudenko, M. Meyer, R. Santra, and T. Jahnke, "X-ray multiphoton-induced Coulomb explosion images complex single molecules," Nat. Phys. **18**(4), 423–428 (2022).
[59]Y. Xu, Y. Huang, and B. Zhang, "Rational design of semiconductor-based photocatalysts for advanced photocatalytic hydrogen production: The case of cadmium chalcogenides," Inorg. Chem. Front. **3**(5), 591–615 (2016).
[60]V. Zalyhina, V. Cheprasova, V. Belyaeva, and V. Romanovski, "Pigments from spent Zn, Ni, Cu, and Cd electrolytes from electroplating industry," Environ. Sci. Pollut. Res. **28**(25), 32660–32668 (2021).
[61]G. F. Nordberg, A. Bernard, G. L. Diamond, J. H. Duffus, P. Illing, M. Nordberg, I. A. Bergdahl, T. Jin, and S. Skerfving, "Risk assessment of effects of cadmium on human health (IUPAC Technical Report)," Pure Appl. Chem. **90**(4), 755–808 (2018).
[62]J. Z. Niecko, "Waste-free method of cadmium carbonate production," Stud. Environ. Sci. **23**, 485–490 (1984).
[63]J. J. Kim, S. S. Lee, P. Fenter, S. C. B. Myneni, V. Nikitin, and C. A. Peters, "Carbonate coprecipitation for Cd and Zn treatment and evaluation of heavy metal stability under acidic conditions," Environ. Sci. Technol. **57**(8), 3104–3113 (2023).